

# **HiSST: 4th International Conference on High-Speed Vehicle Science Technology** 22 -26 September 2025, Tours, France



# Design methodology for a plenum chamber integrated in a Mach 2 blow down wind tunnel using CFD simulation

OUOC-HUY Nahiem1, TRUONG-GIANG Nauven1, DUY-LINH Doil and PHI-MINH Nauven1

#### **Abstract**

This paper describes the design methodology for a plenum chamber in an intermittent blow down wind tunnel (BWT) used to test Ramjet engines. A plenum chamber is a common aerodynamic device in wind tunnels that stabilizes the flow, brings it to a positive pressure, and then delivers a more uniform flow distribution at the throat's outflow. In this study, a Plenum chamber will be designed for an Lshaped wind tunnel to house a Ramjet engine with an inlet diameter of 395 mm at sea level. In addition, some air flow stabilizers (AFS) are integrated into the system to improve flow quality before it is discharged into the environment.

**Keywords**: ramjet, test cell, wind tunnel, plenum chamber.

#### 1. Introduction

Altitude test facilities (ATFs) constitute specialized infrastructure engineered to replicate high-altitude flight conditions within a controlled ground environment. These facilities facilitate the comprehensive evaluation of propulsion system performance across a spectrum of simulated atmospheric conditions, encompassing the entirety of an engine's operational envelope [1] [2]. Among the various types of ATFs, the sea-level blow down wind tunnel (BWT) represents a targeted approach for reproducing sealevel flight scenarios through the generation of high-velocity air jets derived from pressurized air reservoirs [3] [4].

In contrast to more complex ATF systems capable of simulating a wide range of altitudes, sea-level BWTs provide an economically advantageous solution for achieving essential testing objectives under standard atmospheric conditions. Although inherently constrained to sea-level simulations, BWTs are instrumental in conducting rapid engine start procedures, assessing windmilling and slam acceleration phenomena, and evaluating engine-inlet compatibility within rigorously controlled and repeatable flow environments. The capability of these tunnels to produce highly subsonic and supersonic free-stream flows - reaching velocities corresponding to Mach numbers from 2 to 8 [5] [6] [7] - renders them particularly suitable for the investigation and qualification of ramjet and other high-speed propulsion systems.

Technological advancements in BWT design have progressively enhanced the performance, versatility, and cost efficiency of these facilities. By delivering stable, high-speed airflow within a test cell, sealevel BWTs bridge the gap between benchtop experimentation and in-flight assessment, thereby ensuring propulsion systems are subject to thorough pre-deployment evaluation. This approach accelerates the development timeline for aerospace propulsion technologies and contributes to the improvement of safety and performance metrics by enabling the early identification and mitigation of potential deficiencies during the design and validation phases.

Recognizing these challenges, the central aim of this study is to devise a plenum chamber capable of consistently delivering airflow at Mach 2 under sea-level conditions. Due to spatial limitations within our test facility, the implementation of a straight-line blow down wind tunnel (BWT) extending directly from the compressed air reservoir is not feasible; the available space does not permit the alignment of pipe and aerodynamic equiments in a linear configuration. Consequently, the adoption of an L-shaped flow system is necessitated to accommodate the facility's constraints. As illustrated in Figure 1, this L-shaped

HiSST-2025-303 Page | 1 Copyright © 2025 by author(s) arrangement is achieved through the complex connecting pipes, a turning corner, and the plenum chamber, collectively designed to generate Mach 2 airflow at the throat exit.

However, the presence of an upstream butterfly valve, which regulates the airstream, introduces significant turbulence and pressure deficits, as the flow must traverse a section of reduced cross-sectional area relative to the primary pipeline as shown in Figure 2. This transition results in the formation of shock waves downstream of the valve - a phenomenon that is often neglected in existing research, where computational fluid dynamics (CFD) simulations predominantly assume idealized, uniform inlet conditions. Furthermore, the sudden 90° change in flow direction caused by the L-shaped configuration exacerbates pressure losses in proportion to velocity and introduces additional flow instabilities. These factors collectively contribute to oscillatory behaviour in the airstream, diminishing both its uniformity and quality at the plenum chamber's exit.

To address these challenges, the integration of a plenum chamber presents a robust solution for the stabilization of the airstream within the wind tunnel system. The plenum chamber's design, specifically tailored to achieve consistent and high-quality flow, is critical for overcoming the inherent limitations posed by the L-shaped configuration. In its basic form, a plenum chamber constitutes a pressurized enclosure designed to maintain air (or another working fluid) at a positive pressure differential relative to ambient conditions. Conventionally, it comprises a cylindrical shell of uniform diameter, used to balance pressure and facilitate a more uniform distribution of flow, thereby compensating for supply or fluctuations. [3] [4] The substantial internal volume of the chamber results in reduced internal velocities, which is advantageous for flow stabilization. Within the context of wind tunnel and rocket applications, the plenum chamber is strategically positioned upstream in the flow path, and it may also serve as an acoustic silencer. This study proposes a methodology – mainly based on computational fluid dynamics (CFD) simulation - for the design and optimization of a plenum chamber capable of delivering stable, Mach 2 airflow at the chamber outlet. Such a methodological framework ensures the reliability and repeatability of high-speed flow for advanced propulsion testing.

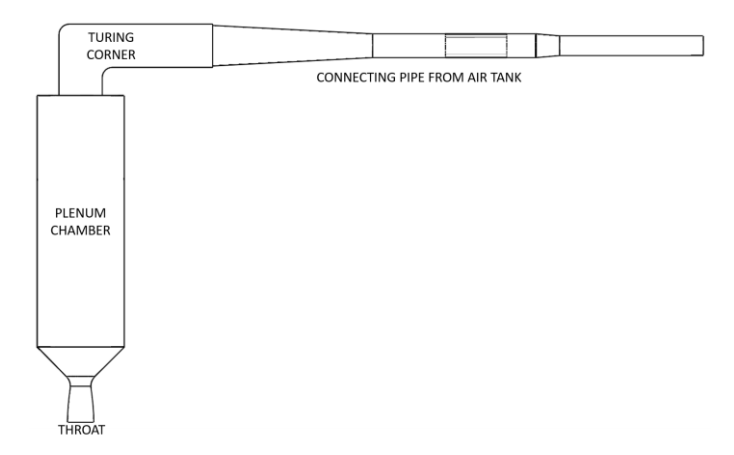


Figure 1. An L-shape blow down wind tunnel design for a limit space of facility.

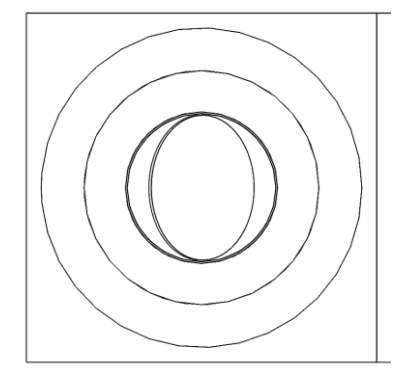


Figure 2. Butterfly valve status when operating.

As mentioned, the inclusion of a butterfly valve within the upstream segment of the flow system not only induces turbulence and pressure losses but also results in an uneven distribution of airflow prior to entry into the nozzle throat. This uneven flow alignment may introduce eccentric loading of the pipeline, thereby generate substantial mechanical stress and serve as a source of structural vibration throughout the wind tunnel assembly. Such vibrational phenomena are hamful to the operational longevity and reliability of the facility.

To eliminate these adverse effects and to ensure superior flow uniformity, the design integrates a set of air flow stabilizers (AFS) within the basic plenum chamber configuration. The downstream section of the butterfly valve incorporates parallel bundle pipes and perforated baffles in the connecting pipe, which serve to decelerate the airstream velocity, while guide vanes are positioned at the turning corner to facilitate a smooth transition of the flow as it enters the chamber and to minimize the potential for flow separation. A square honeycomb is installed before the flow enters the chamber. The plenum chamber itselt includes a non-uniform perforated inverse conical flow. This device functions to redistribute the incoming airflow, thereby promoting a uniform velocity profile prior to passing through a second honeycomb and then the nozzle.

In the following section, the plenum chamber design process is presented and can be divided into two main steps:

- Theoretical and literature-based design: plenum chamber configuration and functional parameters are derived from fundamental fluid dynamic principles and reviewed of relevant literature.
- Aerodynamic optimization: Subsequent refinement of the chamber geometry and the integration of AFS are informed by experimental recommendations and established best practices documented in prior research.

The objective is to realize a plenum chamber capable of supplying a stable, high-quality Mach 2 airflow at the outlet, while simultaneously mitigating vibration and noise attributable to flow disturbances and the implementation of AFS. All proposed design variants are systematically evaluated through computational fluid dynamics (CFD) simulations, ensuring robust operational performance under prescribed conditions and yielding critical insights for ongoing optimisation and practical deployment.

## 2. Materials for design

### 2.1. Performance requirements

This section outlines the principal performance requirements governing the design of a plenum chamber intended to achieve and sustain Mach 2.0 airflow, specifically for the purposes of ramjet engine testing with test object diameters extending up to 500 mm, under the spatial constraints of the experimental facility.

- **Testing Duration:** The system must be capable of delivering an operational interval of no less than 30 seconds for each intermittent test, thereby affording adequate time for precise measurement and systematic data acquisition [4] [8]
- **Target Mach number:** The design objective is the realization of Mach 2.0 airflow at the outlet, under a stipulated condition of 7.8 bar absolute pressure at sea level, thereby closely replicating typical propulsion scenarios encountered in real-world applications.
- **Nozzle Specifications:** The exhaust subsystem incorporates a convergent-divergent (CD) nozzle characterized by a throat diameter of 600 mm (corresponding to 1.2 times the diameter of the test article), with an emphasis on maintaining the stability and uniformity of high-speed flow within the Mach 2 regime.
- Aerodynamic Quality: The delivered flow must exhibit a high degree of uniformity and low turbulence intensity, with minimal fluctuations in velocity and pressure, to guarantee consistent boundary conditions for ramjet engine evaluation.
- Storage: the facility is equipped with high-capacity pressure vessels providing a collective storage volume of approximately 2000 m<sup>3</sup>. These vessels are integrated with the main flow system via DN450 pipes. Furthermore, the modular configuration of the vessel array enables

the parallel augmentation of storage capacity, thereby proportionally extending the duration of each test as necessitated by evolving research requirements.

#### 2.2. CFD method

To assess the aerodynamic characteristics and flow quality, computational fluid dynamics (CFD) analyses are performed utilizing ANSYS FLUENT 19.1. Within the simulation framework, specific physical components - namely, the air storage vessels, DN450 interconnecting pipelines, and all control valve assemblies except for the disk and are intentionally excluded to simpify the computational model. The explicit modeling of the full honeycomb structure is also omitted; such a representation would substantially increase the mesh complexity and computational expense due to the enormous of cell faces and elements. Instead, a representative target plane is introduced at the located honeycomb position within the chamber. By monitoring the flow parameters immediately upstream of this representative plane, the simulation yields a conservative estimate of flow uniformity, with the understanding that the actual conditions will likely result further improvement downstream of the real honeycomb structure.

To evaluate the quality of airflow within the system, in addition to Mach number and total pressure, two principal parameters are systematically analyzed at each cross section, that are the turbulence intensity (TI) and the uniformity index (UI). Turbulence intensity quantitatively characterizes the magnitude of velocity fluctuations present in the flow field; elevated levels of TI are indicative of increased turbulence, which can, in turn, contribute to augmented frictional losses and a at the same time rise in pressure drop throughout the system, thereby potentially compromising operational performance. Conversely, the uniformity index serves as a quantitative measure of the consistency of velocity distribution across a specified cross section of the plenum chamber. Attaining a high degree of flow uniformity is particularly advantageous, as it ensures stable boundary conditions, minimizes pressure losses, and, in configurations involving a heater, substantially improves the efficacy of heat transfer and mixing. The precise determination and monitoring of these parameters are essential for a comprehensive assessment of the aerodynamic performance of the plenum chamber design. The calculation of both metrics utilizes established analytical expressions, as delineated below [9] [10]:

(1) Turbulence Intensity: 
$$I = \frac{u'}{U} \sqrt{\frac{\frac{2}{3}k}{U}} = \frac{\sqrt{\frac{1}{3}(u_x'^2 + u_y'^2 + u_z'^2)}}{\sqrt{U_x^2 + U_y^2 + U_z^2}}$$

(2) Uniformity Index: 
$$\gamma = 1 - \frac{\int_{A_0} v dA}{2V_{avg}A_0}$$

Figure 3 following presents the simulation domain of the fluid as established during the design process, capturing the boundaries of the model.

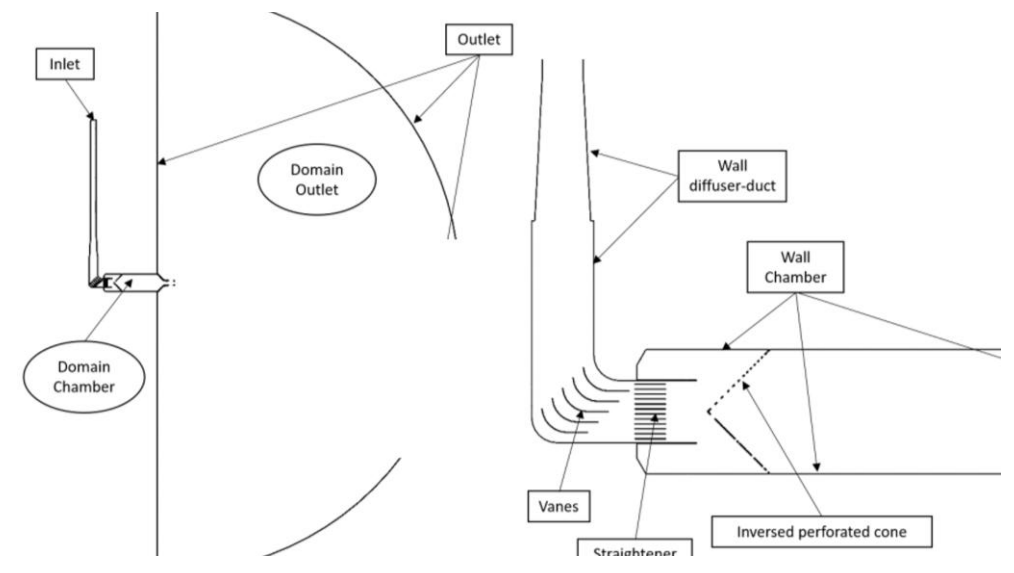


Figure 3. CFD simulation domain and boundaries.

The model is processed and meshed to obtain the hybrid poly-HEXA elements. This approach reduces the number of elements in comparison to the method in which only tetra element is used. Body of influence and face sizing are used for the volume and surface, ensuring precise control over mesh refinement in critical regions such as near the nozzle throat, cone, straightener... The growth rate of elements is maintained at 1.1, allowing for gradual transitions in element size to reduce numerical diffusion and improve solution accuracy. Eight layers of inflation are incorporated to accurately capture boundary layer effects along solid surfaces, providing enhanced resolution of velocity and temperature gradients near the wall. The final mesh structure in chamber is shown in Figure 4.

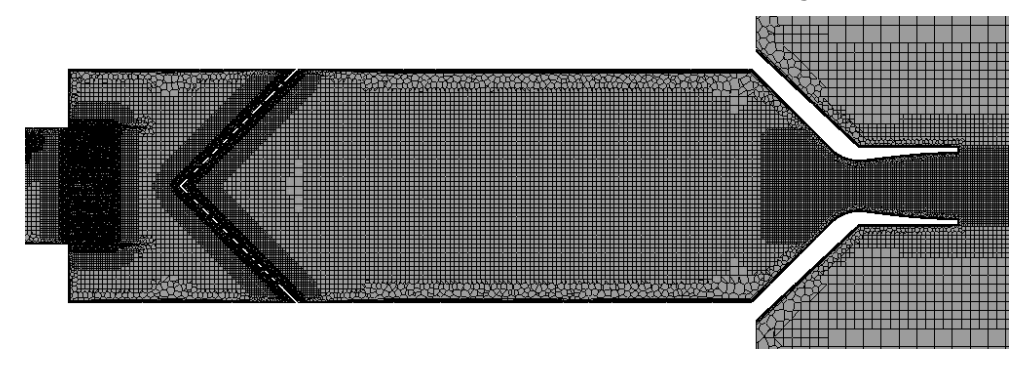


Figure 4. Mesh in poly-hexa core structure inside the chamber.

Preliminary mesh independence studies reveal that the simulation results remain unchanged when the total element count exceeds 14 million, confirming the robustness and reliability of the meshing strategy. The 3D Navier-Stokes equations are solved using the ANSYS FLUENT solver, with the k-ω SST turbulence model employed for closure. This model is particularly chosen for its capability to resolve complex flow separation and near-wall turbulence phenomena, which are expected within the highspeed, high-Revnolds-number environment of the system. The working fluid is modeled as an ideal, compressible air, enabling accurate prediction of shock structures, expansions, and pressure waves that are characteristic of supersonic flow regimes.

During the CFD process, residuals for continuity and momentum equations are monitored to ensure convergence, and key flow parameters, such as Mach number, total pressure, turbulence intensity, and uniformity index, are monitored at the target plane and the throat cross section. These data points allow for a detailed assessment of uniformity and facilitate direct comparison with many configurations of plenum chamber design.

Additional attention is devoted to the validation of the simplified model boundaries. Inlet boundary conditions are applied as specified mass flow and total temperature, replicating the expected upstream storage vessel conditions. Outlet boundaries are defined as ambient pressure to represent sea-level operating condition. The following Table 1 summarizes the boundary conditions, which can be refered to following section 3.1.

Boundary	Туре	Value
Inlet	Mass flow	230 (kg/s)
	Total temperature	267 (°C)
Outlet	Ambient pressure	1 (atm)
Valve, straighteners, diffuser, pipe, corner, vane, sq-honeycomb, chamber, cone, baffle, throat	No slip, adiabatic wall	

Table 1. Boundary condition for the plenum chamber.

## 3. Design plenum chamber

## 3.1. Plenum chamber and throat design

The configuration of the plenum chamber is based on the foundational equations governing isentropic flow, as expressed in equations (3) through (7) [9] [11]. By applying these relationships, the dimensions and operational parameters of the chamber are quickly established to ensure the appropriate balance among pressure, temperature, and velocity. This careful balancing expects a uniform flow field at the throat exit.

(3) Pressure ratio: 
$$\frac{p}{p_t} = \left(1 + \frac{\gamma - 1}{2}M^2\right)^{-\frac{\gamma}{\gamma - 1}}$$

(4) Temperature ratio: 
$$\frac{T}{T_t} = \left(1 + \frac{\gamma - 1}{2}M^2\right)^{-1}$$

(5) Density ratio: 
$$\frac{\rho}{\rho_t} = \left(1 + \frac{\gamma - 1}{2}M^2\right)^{-\frac{1}{\gamma - 1}}$$

(6) Area ratio: 
$$\frac{A}{A^*} = \left(\frac{\gamma+1}{2}\right)^{-\frac{\gamma+1}{2(\gamma-1)}} \frac{\left(1+\frac{\gamma-1}{2}M^2\right)^{\frac{\gamma+1}{2(\gamma-1)}}}{M}$$

(7) Mass flow rate: 
$$\dot{m} = \frac{p_t A^*}{T_t} \sqrt{\frac{\gamma}{R}} \left(\frac{\gamma+1}{2}\right)^{-\frac{\gamma+1}{2(\gamma-1)}}$$

Drawing upon the governing equations of isentropic flow, the principal parameters of the plenum chamber are defined. Under sea-level conditions (1 bar, 27°C), the system achieves a pressure ratio of 7.8 and a total temperature of 267°C. To realize a Mach number of 2 with a nozzle diameter of 600 mm, the critical area (A\*) is calculated to be 460 mm², yielding a system discharge mass flow rate of 230 kg/s, guided by the requisite exhaust velocity and throat dimension.

The primary function of the plenum chamber is to condition and stabilize the airflow preceding acceleration through the convergent-divergent nozzle. In this region, static pressure predominates, and it is reasonable to consider that total pressure closely approximates static pressure. According to the methodology outlined by Pope [4], optimal flow velocities within the plenum chamber are maintained between 10 and 80 ft/s (24-30 m/s). Given the total pressure ratio of 7.8 at Mach 2, the design maintains a Mach number in the plenum chamber between 0.1 and 0.3 to mitigate compressibility effects and prevent the formation of shock waves. In alignment with these criteria, the chamber diameter is set at 2.1 m, corresponding to an internal flow velocity of 13 m/s. In order to optimize flow stabilization and noise reduce within the system, the length of the plenum chamber is determined to be approximately three to four times its diameter [3]. This configuration also accommodates the integration of three AFS designed to further enhance airflow quality. Comprehensive design iterations and CFD analyses have substantiated the adequacy of this sizing approach, leading to the retention of the selected chamber dimensions in all subsequent design versions.

To achieve Mach 2 at the throat, it is crucial to install a nozzle at the end of the plenum chamber. The CD nozzle, which features a tightened middle section followed by a gradual expansion, is particularly well-suited for this task. This nozzle design accelerates compressible fluid to supersonic speeds. CD nozzles are commonly found in steam turbines, rocket engines, and certain jet engines, where their effectiveness relies on the unique behaviors of subsonic, sonic, and supersonic flows. A combined circular arc and Method of Characteristics (MOC) curve configuration has been adopted for the CD nozzle in this BWT to facilitate rapid airflow acceleration while minimizing boundary layer thickness and optimizing the effective area. At the termination of the cylindrical section of the plenum chamber, a conical enclosure with a 90° angle is implemented, Figure 5. In accordance with general recommendations in [12], a circular arc with a diameter of 1.5 time  $D_{A^*}$  is constructed tangentially to the cone. Downstream of the arc, the nozzle contour is extended using a curve derived via the MOC technique, as depicted in Figure 6.

The MOC method, which is widely recognized and utilized in supersonic nozzle design, was originally introduced in [9] and has subsequently been applied in studies such as [5] [6], particularly for the development of supersonic BWT. The design process for the MOC curve is methodical, allowing for precise adjustments through manipulation of two principal parameters: the heat capacity ratio  $\gamma$  and the target outlet Mach number. Generally, these calculations are performed using computational programs to meet specific design criteria. The following Figure 6 presents a representative MOC curve generated using Anderson's methodology [9] and developed with in-house computational code. The illustrated configuration features an outlet diameter of 600 mm and an exhaust nozzle length of 880 mm, conforming to the specified design requirements.

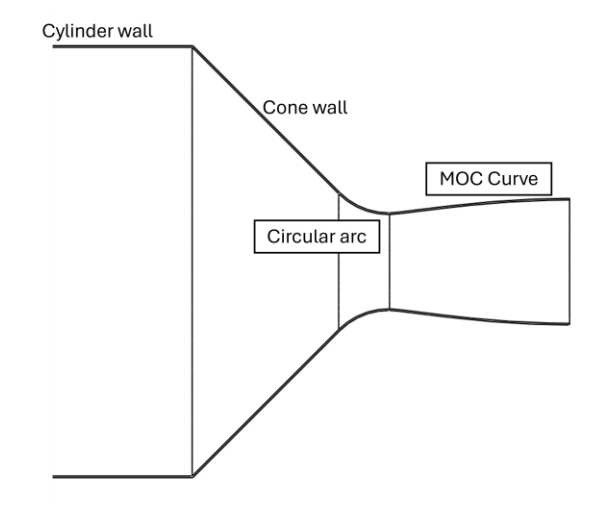


Figure 5. CD nozzle at the end of the plenum chamber.

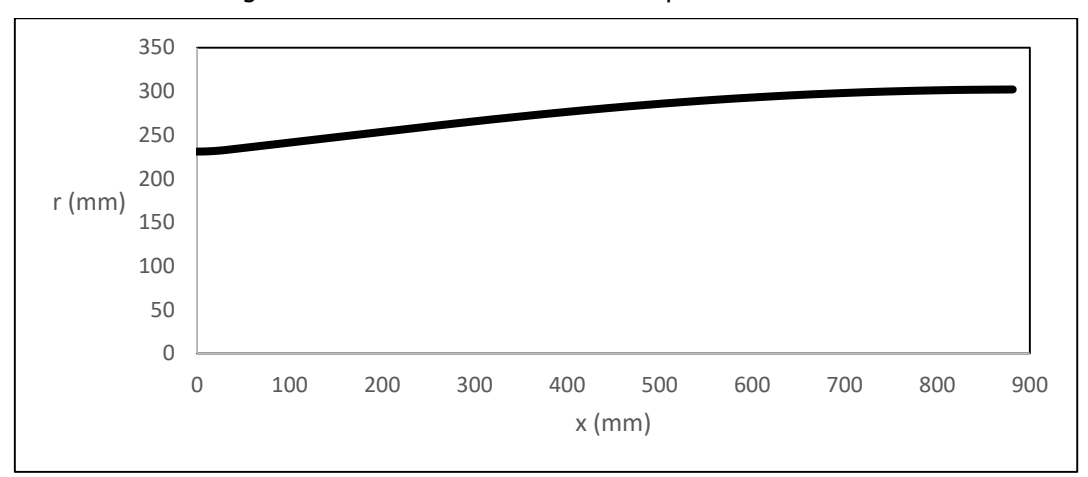


Figure 6. Expansion section of CD nozzle, using Method of Characteristic.

## 3.2. Connecting pipe and turning corner

Upon exiting the compressed air tanks, the airflow is transferred through DN450 connecting pipes and introduced into the system via a butterfly valve. This valve, equipped with adjustable disk, enables fine-tuned regulation of the mass flow rate to achieve the targeted output velocity requisite for system operation. However, each modulation of the valve not only alters the flow rate, but also precipitates a pressure drop in the immediate downstream region. This resultant pressure gradient, in conjunction with the localized constriction at the valve, serves to accelerate the airflow to elevated velocities. Such rapid acceleration of high mass flow rate is conducive to the formation of shock waves which, in turn, engender substantial pressure losses and impair flow stability. The resultant instabilities are further amplified by the increased turbulence and velocity, thereby generating operational noise throughout the system. In sum, while the butterfly valve is integral to precise airflow control, its operational dynamics introduce complex flow phenomena that must be judiciously managed to preserve both the efficiency and acoustic performance of the system.

As noted by Bhatia [13], maintaining pipeline velocity below Mach 0.33 at the outlet is essential for minimizing noise, a consideration that is crucial to aft-valve system design. Similarly, Pope [5] recommends that the Mach number should not exceed 0.4 to prevent the occurrence of whistling noise. Adherence to these established thresholds ensures that the airflow exits the pipe under incompressible conditions, thereby significantly reducing the risk of shock wave formation and associated flow instabilities.

Accordingly, the DN700 pipeline has been selected to fulfill the velocity requirements outlined for the system. To ensure a seamless connection between the DN450 supply pipeline and the main DN700 pipeline, a transitional conical diffuser is incorporated, as depicted in Figure 7. The adoption of this

transition is predicated on its efficacy in eliminating excessive pressure losses resulting from flow separation. Established well-known practices and literature, it is recommended an optimal conical half-angle within the range of 5° to 8°, which offers a balance between minimizing the generation of oblique shock waves and restricting pressure loss, whilst facilitating robust boundary layer control conducive to sustained diffuser performance [14]. Consequently, a cone angle of 8° has been selected to prioritize a more compact diffuser length without compromising system efficiency.

Immediately downstream of this diffuser transition, a perforated baffle in conjunction with an array of flow straightener tubes is incorporated into the system. They are first two parts of AFS integrated into the plenum chamber system as shown in Figure 7. The primary objective of these components is to decelerate the airflow, stabilize the pressure profile within the transitional region, and attenuate any instability induced by the operation of the butterfly valve. The baffle is constructed as a 20 mm thick disc possessing a diameter of 700 mm, perforated with 20 mm holes to achieve an overall permeability of 52%. The bundle of flow straighteners consists of DN120 tubes, each with a length of 1 meter, systematically arranged into a compact matrix through welding. This configuration not only facilitates the uniformity of the velocity field but also contributes to eliminating flow-induced instabilities, thereby enhancing the overall aerodynamic performance of the system. Therefore, rather than connecting the DN450 pipe directly to the DN700 main line, a complex connecting pipe system is implemented to effectively manage the fluctuations caused by the butterfly valve.



Figure 7. Complex connecting pipe system from air vessels to the plenum chamber.

The CFD rusults, as depicted in Figure 8, show the outlet air flow of the connecting pipe system gives a uniform flow quality equivalent to a uniform boundary condition. This is very useful for the design because in the sizing plenum chamber and especially the discharge nozzle using MOC, the quantities are uniformly distributed. This contributes to achieving the target performance at the discharge nozzle outlet. CFD analysis further demonstrates that the UI for both tubes is nearly identical at 98%. However, though the Mach number at the exit of the DN700 pipe is 0.23, accompanied by a 16% pressure loss as a trade-off, while the DN450 pipe exhibits an exit Mach number of 0.76. Additionally, the TI in the DN700 pipe equipped with the AFS is 0.33, which is five times lower than the DN450's value of 1.5%.

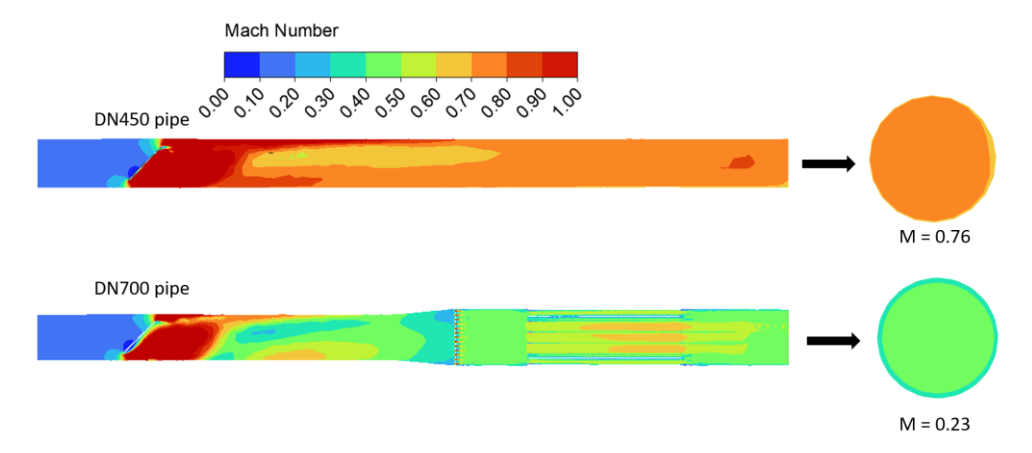


Figure 8. Mach number in the connecting pipe.

Given the spatial constraints for the plenum chamber, an L-shaped configuration in Figure 9 has been adopted. This requires the airflow to make a sharp 90° turn as it enters the plenum chamber. In order to create a seamless transition through the complex connecting pipe and subsequent turning corner, an additional diffuser featuring a 5° cone angle is incorporated in flavor of dealing with high-speed flow. This design strategy is specifically intended to prevent wall separation and to ensure the concentric guidance of airflow as it enters the turning corner region and promotes a more uniform pressure distribution within the turning corner, particularly across the system's guide vanes.

Figure 9. L-shape turing corner with diffuser and guide vane.

Since pressure loss increases by the square of velocity, it is desirable to further decelerate the air after it passes through the connecting pipeline system and before it enters the chamber. Additionally, constructing a large diameter round tube bend (especially of non-standard size, which involves bending and welding) is more complicated than building a square tube, which can be assembled by welding flat steel plates. For this reason, the 90° bend will utilize a square cross-section. The diameter of the plenum chamber, as determined previously, informs the corresponding cross-sectional area of the bend, calculated as  $1.1 \text{m}^2$  with dimensions 1.05 x 1.05 (m). At this stage, computational fluid dynamics (CFD) analysis indicates that the average Mach number in the turning corner drops to 0.09, while peak value is 0.25.

Figure 10 (left) illustrates the outcomes associated with the configuration without the AFS. In this case, the velocity distribution is observed to concentrate proximately to the inner edge of the turning corner, thereby generating a non-uniform pressure field in Figure 11 across the vane surfaces and resulting in elevated stress concentrations on these structural elements. Conversely, as depicted in Figure 10 (right), the integration of the AFS promotes a significantly more uniform and concentric airflow distribution within the diffuser exit region, directing the core flow toward the center of the pipe, which in turn mitigates the occurrence of excessive localized velocities and enhances pressure uniformity across the vanes. Despite these improvements, it is important to note that the substantial inertia of the moving air causes some degree of flow separation at the trailing edge, such that transverse velocity components relative to the primary flow direction are not entirely eradicated.

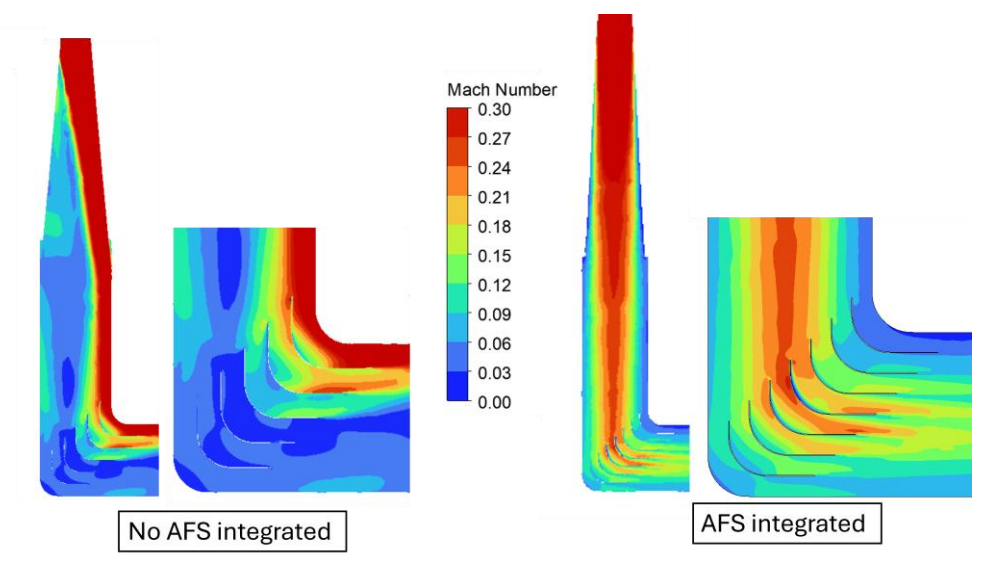


Figure 10. Mach number in the turning corner at case with (left) and without AFS integrated in the connecting pipe.

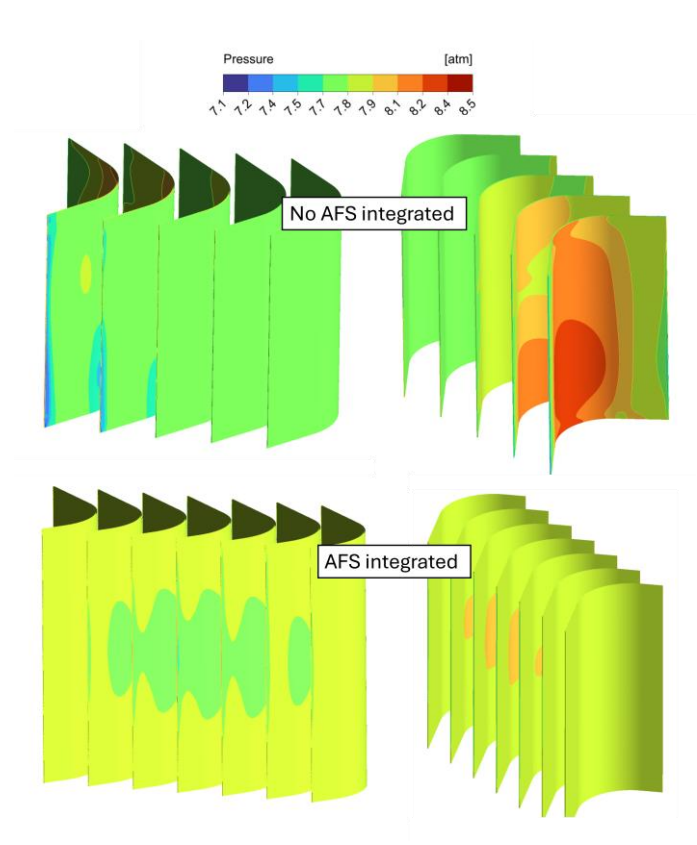


Figure 11. Pressure distribution in guide vane in case with (upper) and without AFS integrated in the connecting pipe.

Through the deliberate design of a complex connecting pipe system to deal with the instabilities introduced by the butterfly valve, and by design the turning corner to effectively decrease the airflow velocity to below Mach 0.1, both noise and vibration may be greatly reduced. As a result, the quality of the airflow upon exiting the turning corner is substantially enhanced compared to configurations lacking the AFS. This improvement is not merely incremental; it plays a crucial role in ensuring that the downstream flow entering the plenum chamber is more uniform and stable. The improved flow characteristics support more effective stabilization, aid in the recovery of static pressure within the chamber and ultimately contribute to the consistent aerodynamic performance of the entire system. This provides a strong foundation for other next AFS including honeycomb structures and perforated cones.

## 3.3. Square honeycomb and perforated cone

To further eliminate the persistence of transverse velocity components following the airflow's passage through the turning corner, a square honeycomb structure is installed immediately downstream. This honeycomb matches the cross-section of the turning corner and cab be made straightforward through the welding of steel bars. The porosity is the most important factor in designing as it effectively minimizes flow fluctuation while reducing associated pressure losses. Bradshaw [15] stated that that wind tunnel screens should have open ratios of 57% or more. Meanwhile, in [16] the authors successfully used a honeycomb with prosity up to 90% in their system. The selection of cell dimensions is selected to ensure a suitable balance among vibration attenuation, structural robustness, and minimal pressure drop. Previous studies in [15] [17] [18] have demonstrated that an optimal ratio of honeycomb length to mesh width (L/D) typically resides within the range of 6 to 8.

Thus, a square honeycomb structure is installed immediately downstream, precisely matching the dimensions of the corner's cross-section at  $1.06 \times 1.06$  meters. Figure 12 depicts the configuration integrated inside the chamber. The honeycomb features a high porosity of 85%, ensuring minimal resistance to airflow while maintaining effective control over flow uniformity. Each cell within the honeycomb is sized at  $80 \times 80$  mm, and the overall length extends to 600 mm, providing a substantial pathway for the air to realign and smooth out turbulence. Constructed from  $8 \times 10^{-10}$  mm thick steel plates

alternately wieled together, the assembly provides both structural integrity and durability under operational stresses.

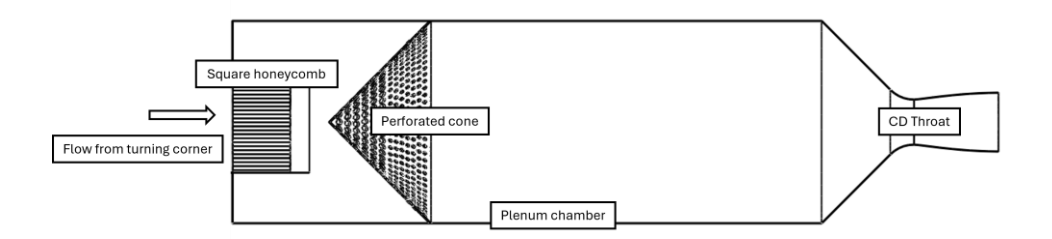


Figure 12. Installation of square honeycomb and perforated cone in the chamber.

Following its passage through the turning corner, the airflow is confined within a square cross-section and subsequently begins to spread, yet a notable concentration remains near the center of the plenum chamber and maximum velocity can reaches up to 60 m/s, as shown on Figure 12 on the left. This phenomenon results in elevated core velocities relative to the peripheral regions, thereby introducing distortion in the velocity profile. It is notable to highlight that a honeycomb mesh is positioned downstream of this region and should the airflow velocity exceed the prescribed design velocity of 13 m/s, such as reaching magnitudes five times higher, acoustic phenomena, including whistling, may be induced. Consequently, achieving a more uniform distribution of airflow within the chamber is imperative to reduce noise.

To accomplish this objective, a specially designed perforated cone with a non-uniform hole pattern is employed to promote uniform airflow at the outlet [4] [19]. The cone, matching the chamber's diameter and set at a 90° angle, is positioned one meter downstream from the square honeycomb with its tip facing the incoming airstream to generate a diffusing effect. As air flows along the cone's surface and passes through perforated holes, it is divided into numerous small jets. These jets then merge behind the cone, reducing overall velocity and increasing static pressure. This process redistributes the flow evenly across the tube's cross-section, ensuring a balanced and stable output.

It is noteworthy that available literature provides limited explicit guidance regarding the optimal design of perforated cones. Accordingly, the present study adopts an empirical, iterative approach, relying on experimental of CFD observations and trial-and-error adjustments. The findings demonstrate that a cone featuring a random arrangement of perforations with varying diameters yields a notably more uniform airflow downstream. Specifically, it is recommended that the perforations occupying one-half of the cone's cross-sectional area possess diameters 1.5 to 2 times larger than those of the perforations on the remaining half. This configuration, as illustrated in Figure 12, effectively enhances the uniformity of the velocity field. Furthermore, to achieve a balance between airflow uniformity, minimized pressure loss, and structural integrity, it is advisable to maintain total cone porosity does not exceed 40±2%.

The proposed perforated cone design features a total of 623 holes, with larger holes, measuring 60 mm in diameter, concentrated at the center, and smaller holes of 35 mm diameter distributed across the remaining area. The overall porosity achieved by this configuration is 26%.

The results at represent target plane at which located the honeycomb is presented in Figure 13. Evidently, the integration of the perforated cone facilitates a more uniform velocity distribution within the chamber (right) when compared to its absence (left). This enhancement also contributes to the attenuation of noise generated by the honeycomb system, underscoring the effectiveness of the perforated cone as an aerodynamic flow management device. The TI at this plane is 0.2%.

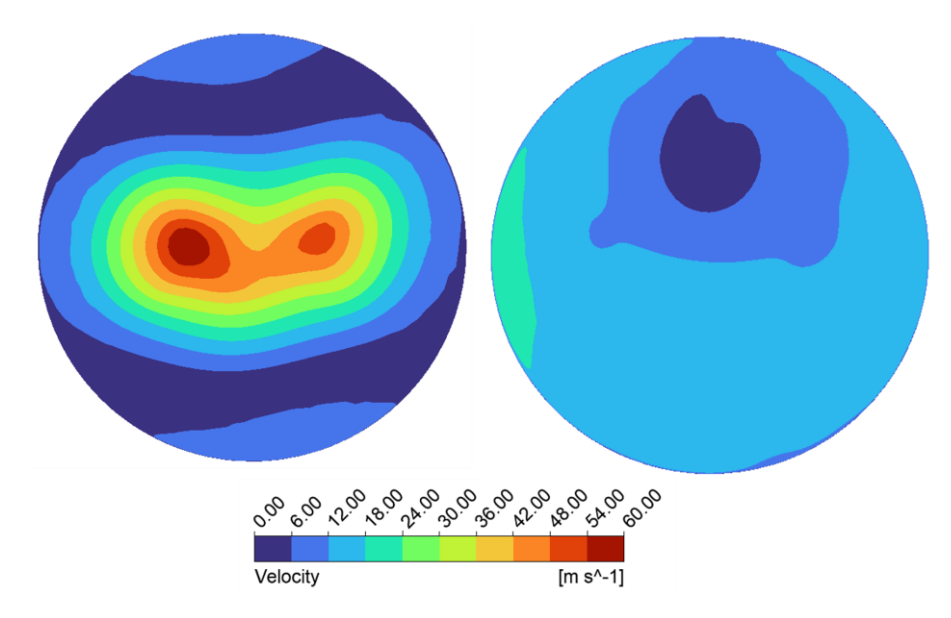


Figure 13. Mach number distribution in representative target plane without (left) and with perforaetd con.

Ultimately, the outcomes at the exhaust are presented in the subsequent figure. At the throat exit, the Mach number attains a value of 2, with the flow field exhibiting a consistently uniform distribution across all assessed configurations, irrespective of initial turbulent conditions, and UI reach 99%, as illusted in Figure 14 and Figure 15. This observation underscores the plenum chamber's capacity to regulate pressure and stabilize incoming turbulent flows. However, the TI of case without AFS is 3 times larger than that of with AFS. This, notably, confirm the integration of these flow management devices demonstrably enhances the quality of airflow within the system, substantially mitigating turbulence induced by upstream elements such as the butterfly valve and the sharp 90° turn. The transition from transient to steady-state flow, coupled with a reduction in velocity to incompressible levels, contributes to diminished vibration and acoustic emissions within the plenum chamber. Such improvements not only facilitate optimal aerodynamic performance but also extend the operational lifespan of the chamber assembly through reduced mechanical stress and noise generation.

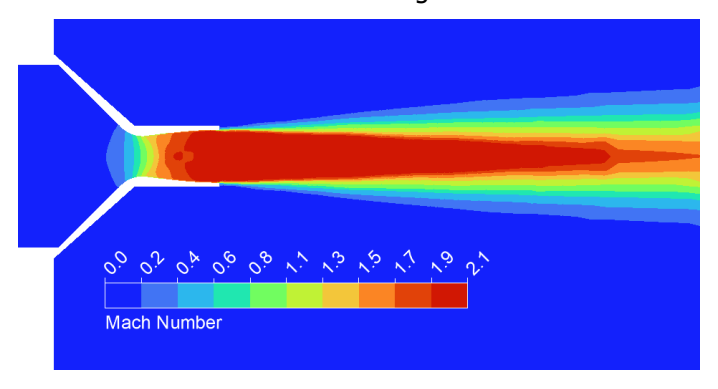


Figure 14. Mach number field at nozzle exit.

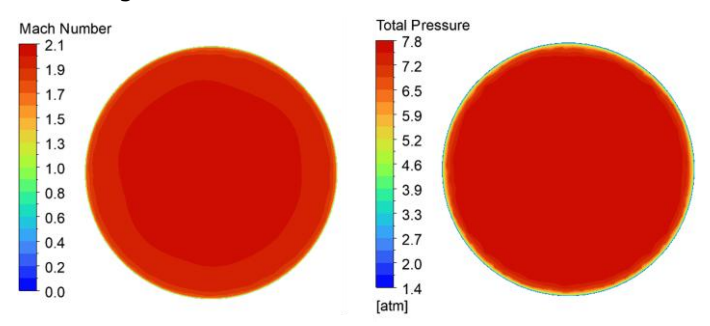


Figure 15. Mach number and Total Pressure distribution at throat plane.

HiSST-2025-303 Q.H. NGHIEM, T.G. NGUYEN

The results obtained from three-dimensional numerical simulations reveal that, although theoretical predictions utilizing the Method of Characteristics (MOC) do not produce an ideal free jet, the flow remains underexpansion condition, with static pressure exceeding atmospheric levels (Ps = 1.05 > 1atm) [11]. Notably, the region proximate to the exhaust nozzle consistently achieves an average Mach number of 2 and a total pressure of 7.8 bar. These findings indicate that the optimal placement of the test specimen is near the nozzle exit. Furthermore, CFD methodologies may be employed to examine the interaction between the exhaust nozzle and the ramjet inlet, thereby enabling the determination of an appropriate gap distance for experimental testing prior to conducting physical trials.

## 4. Conclusion

The study outlines the design process for a plenum chamber used in an intermittent blowdown wind tunnel designed for Ramjet engine testing. Specifically, the chamber is intended for a Ramjet engine with an inlet diameter of up to 500 mm at sea level and is designed to fit an L-shaped wind tunnel due to spatial limitation. Key steps in the design include determining the chamber dimensions and integrating aerodynamic flow stabilizer in the system. Computational Fluid Dynamics simulations are utilized to refine the chamber's performance, ensuring it can withstand high pressure and high turbulent conditions to deliver stable, uniform airflow. Future experimental validation is planned to confirm the simulations' accuracy and to further adjust the CFD models, particularly for studying the interaction between the plenum chamber and the ramjet engine inlet. The effective deployment of this chamber is expected to improve the efficiency and reliability of wind tunnel experiments, providing data for the research of Ramjet engine.

References

- [1] N. D. Grannan, K. J. Moosmann, J. L. Hoke, M. J. McClearn and F. R. Schauer, "Small Turbojet Altitude Test Facility with Two Stage Turbocharger Inlet Air Cooling," in 2018 AIAA Aerospace Sciences Meeting, Florida, 2018.
- [2] C. Kim, M. Yoon, S. Yang and D. Lee, "An altitude test facility for small jet engines," in 37th Joint Propulsion Conference and Exhibit, Salt Lake, 2001.
- [3] I. E. Beckwith, "Comments on settling chamber design for quiet, blowdown wind tunnel," NASA,
- [4] A. Pope and K. L. Goin, High Speed Wind Tunnel Testing, Wiley, 1965.
- [5] B.-K. Sung and J.-Y. Choi, "Design of a Mach 2 shape transition nozzle for lab-scale direct-connect supersonic combustor," Aerospace Science and Technology, vol. 117, 2021.
- [6] A. W. Fiore, D. G. Moore, D. H. Murray and J. E. West, "Design and Calibration of the ARL Mach 3 High Reynolds Number Facility," 1972.
- [7] P.A.Jacobs and R.J.Stalker, "MACH 4 AND MACH 8 AXISYMMETRIC NOZZLES FOR A SHOCK TUNNEL," 1991.
- [8] DNW, "Supersonic blowdown wind tunnel," DNW, [Online]. Available: www.dnw.aero/windtunnels/sst/. [Accessed Aug 2025].
- [9] J. D. Anderson, Fundamentals of Aerodynamics, McGraw Hill, 2016.
- [10] F. S. Marincowitz, M. T. F. Owen, J. Muiyse and P. Holkers, "Uniformity Index as a universal aircooled condenser performance metric," International Journal of Turbomachinery Propulsion and Power, 2022.
- [11] G. P. SUTTON and O. BIBLARZ, Rocket Propulsion Elements, John Wiley & Sons, 2001.
- [12] G. V. R. Rao, "Exhaust nozzle contour for optimum thrust," Jet propulsion, 1958.
- [13] A. Bahatia, Control Valve Basics: Sizing and Selection, CEDEngineering.
- [14] A. Lefebvre and D. Ballal, "Gas turbine combustion: alternative fuels and emissions," CRC press.
- [15] P. Bradshaw, "The effect of wind-tunnel screens on nominally two-dimensional boundary layers," Journal of Fluid Mechanics, vol. 22, no. 4, pp. 679 - 687, 1965.
- [16] P. Patel and S. G. Aggarwal, "Theoretical and Experimental Evaluation of a Compact Aerosol Wind-tunnel and its Application for Performance Investigation of Particulate Matter Instruments," Aerosol Physics and Instrumentation, 2021.
- [17] J. Barlow, W. Rae and A. Pope, Low-speed wind tunnel testing, John wiley & sons, 1999.

- [18] J. Scheiman, "Considerations for the installation of honeycomb and screens to reduce wind-tunnel turbulence," NASA, 1981.
- [19] A. Ferri and S. Bogdonoff, Design and operation of intermittent supersonic wind tunnels, North Atlantic Treaty Organization, Advisory Group for Aeronautical Research and Development.
- [20] C.-G. Li, J. C. K. Cheung and Z. Chen, "EFFECT OF SQUARE CELLS IN IMPROVING WIND TUNNEL FLOW QUALITY," in *The Seventh Asia-Pacific Conference on Wind Engineering*, Taiwan, 2009.
- [21] R. D. MEHTA and P. BRADSHAW, "Design rules for small low speed wind tunnels," Cambridge, 1979.